

PDF hosted at the Radboud Repository of the Radboud University Nijmegen

The following full text is a publisher's version.

For additional information about this publication click this link.

<http://hdl.handle.net/2066/107957>

Please be advised that this information was generated on 2017-12-06 and may be subject to change.

ORIGINAL ARTICLE

Functional MRI techniques demonstrate early vascular changes in renal cell cancer patients treated with sunitinib: a pilot study

I.M.E. Desar^a, E.G.W. ter Voert^b, Th. Hambroek^b, J.J.A. van Asten^b, D.J. van Spronsen^c,
P.F.A. Mulders^d, A. Heerschap^b, W.T.A. van der Graaf^a, H.W.M. van Laarhoven^a and
C.M.L. van Herpen^a

^aDepartment of Medical Oncology, Radboud University Nijmegen Medical Centre, Nijmegen, The Netherlands;
^bDepartment of Radiology, Radboud University Nijmegen Medical Centre, Nijmegen, The Netherlands; ^cDepartment
of Internal Medicine, Canisius Wilhelmina Hospital, Nijmegen, The Netherlands; ^dDepartment of Urology,
Radboud University Nijmegen Medical Centre, Nijmegen, The Netherlands

Corresponding address: I.M.E. Desar, Department of Medical Oncology 452, Radboud University Nijmegen Medical
Centre, PO Box 9101, 6500 HB Nijmegen, The Netherlands.
Email: i.desar@AIG.umcn.nl

Conflicts of interest: Prof. P.F.A. Mulders receives minor honoraria from Pfizer and AstraZeneca.

Funding: none.

This study has been presented in a poster session during the ASCO annual meeting 2010 in Chicago
and during the ISMRM annual meeting 2010 in Stockholm.

Trial registration number: NCT00509704

Date accepted for publication 3 October 2011

Abstract

Objective: To assess the early vascular effects of sunitinib in patients with renal cell carcinoma (RCC) with diffusion-weighted magnetic resonance imaging (DWI), dynamic contrast-enhanced (DCE) magnetic resonance imaging (MRI) and T2* perfusion MRI. **Patients and methods:** In 10 patients with abdominal RCC lesions, DWI, DCE-MRI and T2* perfusion MRI measurements at 3 Tesla were performed at baseline, 3 and 10 days after start of sunitinib. VEGF-A plasma levels were measured on days 0, 3 and 10. **Results:** DWI showed a significant increase in the apparent diffusion coefficient ($\times 10^{-6}$ s/mm²) from baseline (mean 1158, range 814–2003) to day 3 (mean 1306, range 1008–2097, $P=0.015$) followed by a decrease to baseline levels at day 10 (mean 1132, range 719–2005, $P=0.001$). No significant changes were found in mean DCE-MRI parameters. T2* perfusion MRI showed a significant decrease in relative tumor blood volume (rBV) and relative tumor blood flow (rBF) at day 3 (rBV $P=0.037$, rBF $P=0.018$) and day 10 (rBV $P=0.006$, rBF $P=0.009$). VEGF-A plasma levels significantly increased after 10 days, but did not correlate with MRI parameters. **Conclusions:** Sunitinib induces antiangiogenic effects as measured by DWI and T2*-perfusion MRI, 3 and 10 days after the start of the initial treatment. DCE-MRI did not show significant changes. In the near future, early functional MRI-based evaluation can play an important role in tailoring treatment to the individual patient with RCC. Further investigation is warranted.

Keywords: Sunitinib; renal cell carcinoma; dynamic contrast-enhanced magnetic resonance imaging; diffusion-weighted magnetic resonance imaging; T2* perfusion magnetic resonance imaging.

Introduction

Angiogenesis is essential for the growth and metastases of tumors. Several angiogenesis inhibitors are registered for the treatment of metastatic renal cell carcinoma (mRCC), including sunitinib^[1,2]. There is a great need to predict clinical outcome early after the start of sunitinib treatment in order to optimize treatment schedules and prevent unnecessary toxicity and costs. Size changes as assessed by computed tomography (CT) scans according to the Response Evaluation Criteria for Solid Tumors (RECIST) guidelines^[3] cannot be expected in this early phase. Therefore, new predictive and reliable biomarkers, are needed^[4].

Several functional magnetic resonance imaging (MRI) techniques are attractive as early predictors of response to sunitinib treatment. Dynamic contrast-enhanced MRI (DCE-MRI) is a noninvasive functional imaging technique that can be used to measure the properties of the tumor microvasculature in vivo. T1 sequences sensitive to the presence of contrast medium in the extravascular extracellular space (EES) can provide information on microvessel perfusion, permeability, and extracellular leakage space^[5]. Diffusion-weighted MRI (DWI) provides information about the random (Brownian) motion of water molecules. The movement of water molecules in the extracellular space is modified by interactions with cell membranes and macromolecules. Therefore, DWI can be used to monitor cellularity and necrosis. Information about tumor blood volume and tumor blood flow can be obtained with T2*-perfusion MRI after a second administration of contrast. This is based on the assumption that the first bolus of contrast saturated the EES^[6]. This pilot study aims to assess the early vascular changes in RCC lesions induced by sunitinib using DCE-MRI, DWI and T2* perfusion MRI at 3 Tesla.

Methods

Patients

Ten patients with RCC planned for sunitinib treatment who had progressive RCC lesions of at least 2 cm in diameter in the liver, kidneys, abdominal lymph nodes or intra-abdominal soft tissue were included. Both the 50 mg once daily 4 weeks on/2 weeks off schedule as well as the 37.5 mg once daily continuously schedule were accepted. Exclusion criteria were comparable with the usual exclusion criteria for contrast MRI, including a glomerular filtration rate <30 ml/min/1.73 m². Prior systemic treatment including other tyrosine kinase inhibitors (TKIs) was allowed provided that it had been stopped because of progressive disease at least 2 weeks before study entry. CT response evaluation was performed every 2 cycles of treatment according to RECIST. The results of the functional imaging techniques measured on day 0, 3 and 10 of the first cycle, were compared with the

RECIST evaluation after the first 12 weeks of treatment (2 cycles). This RECIST evaluation and the functional imaging analyses were performed by the same observer. All patients gave written informed consent. The study was approved by the medical ethical committee.

DWI, DCE-MRI and T2-perfusion MRI data acquisition*

DWI, DCE-MRI and perfusion MRI were performed at baseline, and at 3 and 10 days after the start of the first sunitinib treatment cycle. These time points were chosen based on the hypothesis of time-dependent changes in tumor vascularization during treatment with angiogenesis inhibitors, starting with normalization of the vasculature and ending with loss of vasculature and necrosis^[7].

Measurements were performed on a 3.0-T Siemens Magnetom Trio MR system (Siemens, Erlangen, Germany), using body phased array receive coils. After conventional T1- and T2-weighted imaging, echo-planar DWI was obtained during 22-s breath holds after maximal expiration, using 3 gradient factors ($b = 50$, $b = 300$ and $b = 600$ s/mm²). This was repeated 3 times in exactly the same way. Sequence parameters were: resolution time 1800 ms, echo time 62 ms, field of view 360×317 mm, matrix 100×88 , 13 slices of 10-mm thickness, fat suppression and parallel factor 2.

Proton density weighted images were acquired with the same sequence parameters as the DCE-MRI except for a flip angle of 10° and repetition time (TR) 250 ms. DCE-MRI was performed after administration of 15 ml of 0.5 M gadolinium (Gd)-DOTA (Dotarem, Schering, Berlin, Germany) intravenously (iv) in 6 s by a SpectrisTM MR injection system. Using a two-dimensional T1-weighted fast low-angle shot (FLASH) gradient echo sequence with a time resolution of 2 s, Gd-DOTA uptake in the tissue was monitored during 5 min. A vascular normalization function (VNF) was determined from pixels in the spleen^[8,9]. Sequence parameters were: TR 39 ms, echo time (TE) 2.08 ms, α 45°, field of view 350×263 mm, matrix 256×103 , slice thickness 7 mm, 8 slices.

After the dynamic T1 measurements, a second bolus of 15 ml of 0.5 M Gd-DOTA was administered iv in 3.75 s followed by dynamic T2* weighted echo-planar measurements during 90 s in order to measure perfusion^[10]. Sequence parameters were: TR 1000 ms, TE 23 ms, α 90°, field of view 320×180 mm, 4 slices of 10 mm.

For follow-up scans, slice positions were matched with the first session using anatomic hallmarks as a reference.

Data analysis

DWI

To improve the DWI results DWI measurements were repeated 3 times at each time point. At a tumor level that was adequately imaged at all 9 occasions, a two-dimensional region of interest (ROI) was drawn to include the

whole tumor and regions of presumed necrosis. At every time point, for each tumor level, a mean apparent diffusion coefficient (ADC) map was calculated out of the 3 DWI sequences made at that specific time point. These mean ADC maps were compared for days 0, 3 and 10. ADCs were calculated using Inline diffusion software (Siemens Syngo VB15). All ROIs, including those for DCE-MRI and T2*-perfusion MRI, were drawn by the same observer. Mean ADC map outcomes were averaged for each time point.

DCE-MRI

DCE-MRI data were analyzed according to the pharmacokinetic model and consensus nomenclature essentially as proposed by Tofts et al. were used^[22]. These include: (1) a volume transfer constant K^{trans} (per minute), (2) the volume of the EES per unit volume of tissue v_e , and (3) the flux rate constant between EES and plasma k_{ep} (per minute). The rate constant is the ratio of the transfer constant to the EES ($k_{ep} = K^{trans}/v_e$). Lower values of k_{ep} or K^{trans} can indicate (1) lower perfusion, (2) lower permeability and/or (3) a smaller blood vessel surface area, globally denoting reduced tumor vascularity^[22]. By combining data from the proton density images with the DCE-MRI data, the tissue concentration of Gd-DOTA was estimated^[23]. The relaxivity of Gd-DOTA was assumed to be homogeneously distributed. The spatial distribution of the values of the rate constant k_{ep} and volume transfer constant K^{trans} were represented in a map. ROIs were drawn around all tumor tissue on a T1-weighted MR image, recorded directly before the arrival of Gd-DOTA in the tumor. These ROIs were applied to the maps of k_{ep} and K^{trans} in order to select the single values of k_{ep} and K^{trans} for all tumor pixels. The means of k_{ep} and K^{trans} of the pixels of all slices containing tumor tissue were calculated after log transformation. All pixels with values equal to zero were regarded as fitting errors or necrotic tumor parts and were excluded. Back transformation of this log-transformed average value resulted in an average value of k_{ep} and K^{trans} for the whole tumor^[19]. Histograms of the log-transformed values of k_{ep} and K^{trans} were analyzed as described before^[24,25]. This histogram analysis does not assess changes in mean k_{ep} or K^{trans} values within a tumor ROI, but calculates a low threshold value (TV_{low}) from the formula $[TV = M - 1.96 \times SD]$ and a high TV from the formula $[TV_{high} = M + 1.96 \times SD]$ for k_{ep} and K^{trans} , where M and SD are the mean and the standard deviation values at baseline. After treatment, the number of pixels below TV_{low} and above TV_{high} were compared with baseline. This method provides more information about the heterogeneity within a tumor, which is necessary because tumors may have a necrotic part or a balance in immature and more mature neovasculature.

T2*-perfusion MRI

The T2*-perfusion images were analyzed using the standard Siemens Syngo VB15 software. ROIs were drawn around RCC lesions. Relative tumor blood volume (rBV) (AU) and tumor blood flow (rBF) (AU/s) were determined, enabling the calculation of the mean transit time (MTT) (s) as: $MTT = rBV/rBF$ ^[15,16].

Vascular endothelial growth factor A (VEGF-A)

Baseline and 3 and 10 days after starting sunitinib, blood samples were taken to analyze for VEGF-A. Plasma samples were stored at -80°C within 1 h after venipuncture. Plasma concentrations were measured with the four-antibody sandwich ELISA^[17]. Data were correlated to the MRI parameters.

Statistics

To analyze the change in MRI and blood biomarkers within the 3 time moments, 2-tailed paired t tests were performed on log-transformed values. Log transformation was used because of the limited number of patients. Correlations were determined using the Pearson correlation test and 95% regression and prediction intervals were calculated using SPSS (ver. 16.0). A P value < 0.05 was considered significant. Data on correlations with progression-free survival (PFS) are provided but this study is not powered to reveal the ability of the techniques to predict PFS and should therefore be interpreted cautiously.

Results

Patients

For this pilot study we aimed to include 10 patients with RCC with adequate DWI and DCE-MRI measurements at all 3 time points. Optimization of T2*-perfusion MRI sequences was finalized after the first patients had already started and were therefore available for 8 patients. The baseline characteristics of the 10 patients treated with sunitinib are reported in Table 1. The median PFS was 22 weeks (mean 37 weeks, range 5–115 weeks). Prior cytokine or TKI treatment did not influence the PFS or functional MRI results ($P > 0.1$).

DWI

The mean ADC increased significantly from baseline ($1158 \times 10^{-6} \text{ s/mm}^2$, range 814–2003) to day 3 ($1306 \times 10^{-6} \text{ mm}^2/\text{s}$, range 1008–2097) ($P = 0.015$) followed by a significant decrease on day 10 ($1132 \times 10^{-6} \text{ mm}^2/\text{s}$, range 719–2005) ($P = 0.010$) (Figs. 1 and 2). Neither baseline ADC values nor the change in ADC values were correlated with dynamic T1 and T2* results, or with RECIST results ($P > 0.1$).

Table 1 Baseline patient characteristics ($n = 10$)

Characteristic	
Age (years)	
Median (range)	60 (54–76)
Gender, n (%)	
Male	10 (100)
ECOG, n (%)	
0	9 (90)
1	1 (10)
Prior treatment, n (%)	
Cytokines	2 (20)
Prior TKI	3 (30)
Tumor types, n (%)	
Clear cell carcinoma	8 (80)
Papillary carcinoma	1 (10)
Mixed clear cell/papillary carcinoma	1 (10)
Median tumor diameter, cm (range)	
Liver (%)	5 (50)
Kidney (%)	
Lymph node (%)	3 (30)
Abdominal fat mass (%)	2 (20)
Sunitinib dose, n (%)	
50 mg (4/2 schedule)	8 (80)
37.5 mg (continuous dose)	2 (20)

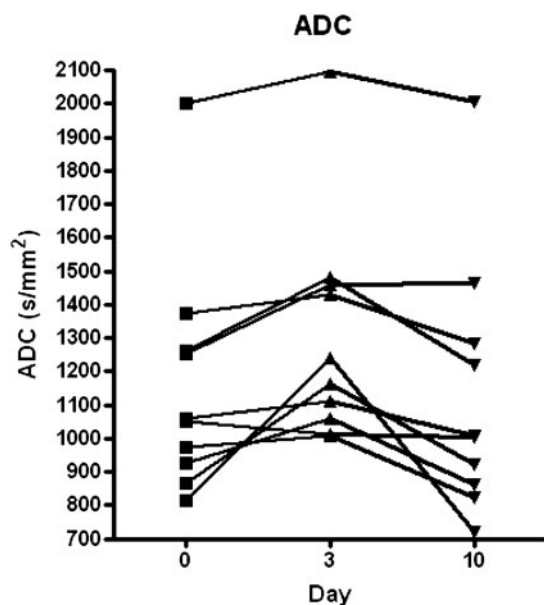


Figure 1 DWI shows a significant increase of ADC ($\times 10^{-6} \text{ mm}^2/\text{s}$) from baseline (mean 1158, range 814–2003) to day 3 (mean 1306, range 1008–2097, $P = 0.015$) followed by a decrease to baseline levels at day 10 (mean 1132, range 719–2005, $P = 0.001$).

DCE-MRI

No significant differences were observed in the mean values for k_{ep} and K^{trans} ($P > 0.1$) (Fig. 1). No correlation was found between the change in k_{ep} and K^{trans} values and response according to RECIST after 2 cycles of treatment. The histogram analyses revealed no significant

changes. The decrease in mean k_{ep} and K^{trans} values after 10 days of sunitinib treatment correlated with prolonged PFS (k_{ep} , $r = -0.598$ and $P = 0.052$; K^{trans} , $r = -0.617$, $P = 0.043$).

$T2^*$ perfusion MRI

The mean rBV significantly decreased from baseline (1019.8 AU, range 412.1–1944.0) to day 3 (721.0 AU, range 55.8–1996.7) ($P = 0.044$) and between baseline and day 10 (573.5 AU, range 99.7–1597.6) ($P = 0.007$) (Fig. 3a). The mean rBF was significantly lower on day 10 (69.2 AU/s, range 12.4–148.1) compared with baseline (154.3 AU/s, range 83.3–290.8) ($P = 0.002$) (Fig. 3b). We observed a decrease in mean MTT from baseline (9.15 s, range 1.5–17.6) to day 3 (6.8 s, range 11.5) ($P = 0.015$) but not from baseline to day 10 (11.5 s, range 4.0–18.4) ($P > 0.1$) (Fig. 3c). Baseline rBV values were correlated with PFS ($r = 0.836$, $P = 0.010$), as did rBV values at days 3 and 10 ($r = 0.736$, $P = 0.037$; $r = 0.0751$, $P = 0.032$, respectively). Baseline rBF and day 10 rBF values also correlated with PFS ($r = 0.739$, $P = 0.036$ and $r = 0.904$, $P = 0.002$) (Fig. 5). The change in rBV or rBF did not correlate with PFS or with RECIST response after 2 cycles of treatment (all $P > 0.1$).

VEGF-A

Mean VEGF-A plasma levels increased significantly from baseline (0.74 ng/ml) to day 3 (0.89 ng/ml) ($P = 0.049$) and between baseline and day 10 (1.41 ng/ml) ($P = 0.010$). VEGF levels were not correlated with DWI, DCE-MRI or perfusion MRI results or with PFS.

Discussion

This is the first study to use 3 functional MRI techniques to assess the early vascular changes in RCC patients induced by sunitinib. As early as 3 days after start of sunitinib, we observed significant increases in ADC, rBV and rBF. In 2010, early response after 15 days of sunitinib treatment in patients with metastatic RCC was observed by dynamic contrast-enhanced ultrasonography^[18]. Furthermore, fluorodeoxyglucose (FDG)-positron emission tomography (PET)/CT has been successfully used to assess the effects of 2–3 cycles of sunitinib treatment in patients with RCC^[19,20].

DWI is able to provide information about cellularity, edema and necrosis. We observed a significant increase of ADC values in RCC lesions after 3 days of sunitinib. This may be caused by the development of necrosis, cell swelling and edema. For chemotherapy, increases in ADC have been reported within days due to cell death with a subsequent increase in extracellular space^[21,22]. We found a subsequent decrease of ADC maps back to baseline values at day 10. This decrease at day 10 compared with day 3 could be explained by tissue

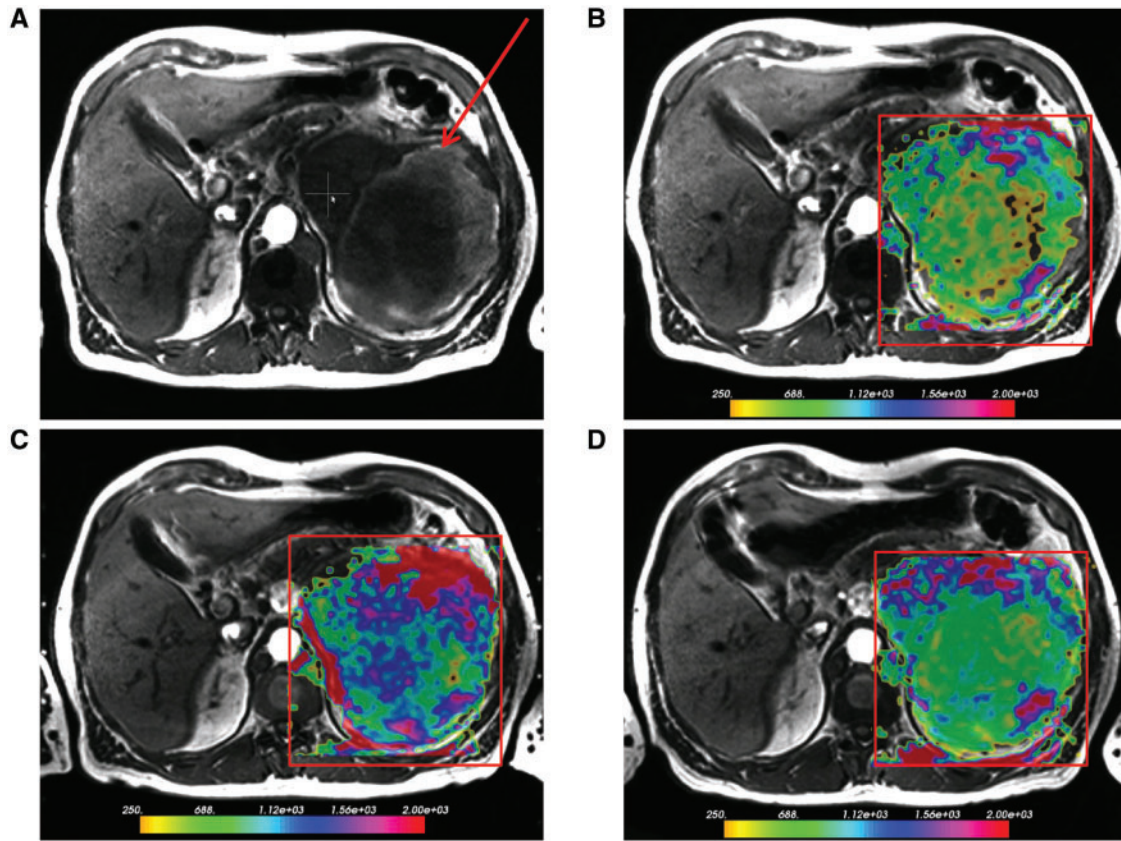


Figure 2 Change in ADC over time. (A) Large tumor in the left kidney visualized by conventional T1 MRI. (B) Baseline ADC map projected on conventional T1 MRI image. Mean ADC value $814 \times 10^{-6} \text{ mm}^2/\text{s}$. (C) Increase in ADC values after 3 days of treatment with sunitinib. Mean ADC value $1239 \times 10^{-6} \text{ mm}^2/\text{s}$. (D) Recovery to baseline ADC values 10 days after starting sunitinib. Mean ADC value $719 \times 10^{-6} \text{ mm}^2/\text{s}$.

dehydration following cell death and by ischemia as a result of decreased blood flow, which was observed by perfusion MRI^[23,24]. A decrease in ADC maps was also noted 2–4 weeks after the start of sorafenib treatment in patients with hepatocellular carcinoma (HCC)^[24]. In that study, treatment-related intralesional hemorrhage was suggested as an explanation for the decrease in ADC. We have no data about changes in ADC after day 10. In the HCC trial, an increase in ADC maps was observed after 2–3 months of sorafenib treatment. Such a re-increase could be explained in cases of sustained cell necrosis leading to enlargement of the extracellular space and thus a loss of diffusion restriction. Only 4 other clinical DWI studies with targeted therapies have been performed previously. In 2 studies the effect of bevacizumab, a monoclonal antibody against VEGF, was assessed. A trend toward an increase in mean ADC values was observed in patients with brain tumors who did not have progression after 1 year of treatment^[25]. In the second study on patients with glioblastoma multiforme (GBM), lower baseline ADC values were associated with a more favorable outcome after 6 months of treatment^[26]. In a third study, the effect of the anti-vascular drug combrestatin A4 phosphate alone as well

as the combination of combrestatin A4 phosphate and bevacizumab was studied in patients with solid tumors. A significant increase in median ADC was observed 3 h after the second administration of combrestatin A4 phosphate, which decreased after the administration of bevacizumab^[27]. In the last study, tumor escape of GBM during treatment with cediranib, a VEGF-receptor inhibitor, was associated with an increase in low ADC areas, which represented growing tumor with increasing cellularity^[28].

In this small pilot study, we did not find significant changes in DCE-MRI parameters after 3–10 days of treatment with sunitinib. We did find some correlations with PFS but in these very small numbers, this should be interpreted with caution. In 2 previous studies, decreases in DCE-MRI parameters after 4–12 weeks of treatment with sorafenib in RCC have been reported^[29,30]. In one of these studies, high baseline K^{trans} was associated with better treatment outcome and the change in K^{trans} correlated with the PFS^[30]. Studies with DCE-MRI and sunitinib have not been performed in patients with RCC before. The vascular effects of sunitinib have been assessed by DCE-MRI in a phase II study in patients with recurrent or metastatic squamous

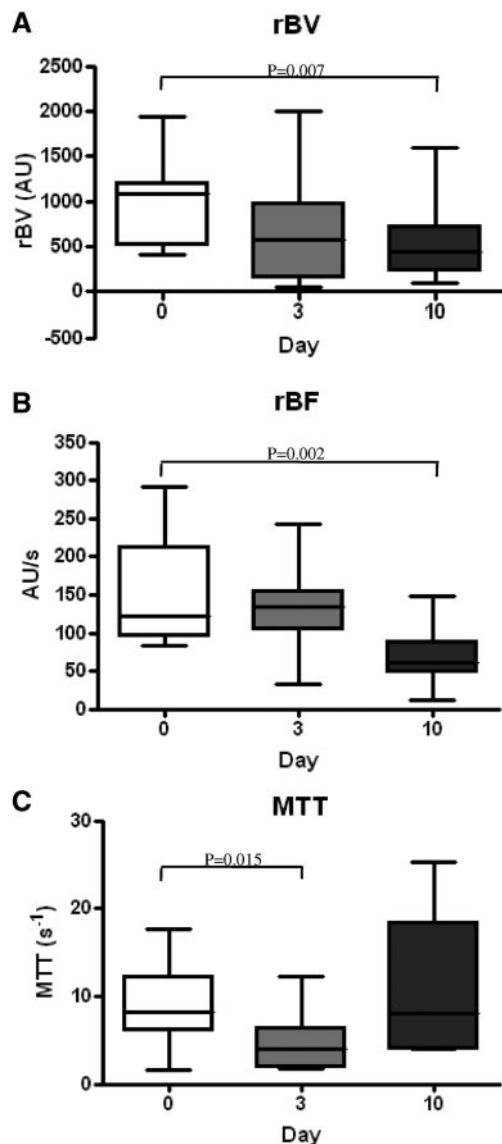


Figure 3 Changes in perfusion parameters, rBV, rBF and MTT. (A) rBV significantly decreased from baseline (mean 1019.8, range 412.1–1944.0) to day 3 (mean 721.0, range 55.8–1996.7) ($P = 0.044$) and between baseline and day 10 (mean 573.5, range 99.7–1597.6) ($P = 0.007$). (B) The relative tumor blood flow (rBF) significantly decreased from baseline (mean 154.3, range 83.3–290.8) to day 10 (mean 69.2, range 12.4–148.1) ($P = 0.002$). This decrease was more pronounced between day 3 (mean 132.8, range 33.1–242.7) and day 10 ($P = 0.003$), not from baseline to day 3 ($P > 0.1$). (C) A decrease in mean transit time (MTT) from baseline (mean 9.15 s, range 1.5–17.6.0 s) to day 3 (mean 6.8 s, range 11.5 s) ($P = 0.015$) but not from baseline to day 10 (mean 11.5 s, range 4.0–18.4 s) ($P > 0.1$) was observed.

cell carcinoma of the head and neck, and a significant decrease in K^{trans} was observed after 6–8 weeks in 3 out of 4 patients^[31]. In HCC patients treated with sunitinib, significant decreases in k_{ep} and K^{trans} were observed after

Table 2 Mean outcomes at baseline, day 3 and 10

	Baseline	Day 3	Day 10	P (day 0 vs 10)
ADC (10^{-6} s/mm ²)	1158	1306	1132	0.010
k_{ep} (/s)	0.0356	0.0255	0.0236	>0.1
K^{trans}	0.02300	0.01706	0.01718	>0.1
rBV (AU)	1020	721	573	0.018
rBF (AU/s)	154	132	69	0.002
MTT (s)	9.15	6.8	11.5	>0.1

14 days, which were more pronounced in responding patients^[32].

Extracranial T2*-perfusion MRI is relatively new. We observed a decrease in rBV and rBF after 3 and 10 days of sunitinib treatment. One could speculate that high baseline rBV and rBF values are determined by high intratumoral VEGF concentrations and may thus be related to treatment response to VEGFR inhibitors. These tumors will be more vulnerable to treatment modalities interfering with the VEGF pathway. The increase in VEGF plasma levels during antiangiogenic treatment is well known and does not reflect intratumoral VEGF levels^[33]. Indeed, we did not find a correlation between VEGF-A plasma levels and functional MRI parameters. However, the values of rBV and rBF as early biomarkers of response to antiangiogenic treatment in cancer patients are still to be determined.

Besides functional MRI, molecular imaging techniques can be of interest in patients with mRCC treated with TKIs. For example, Kayani et al. reported that baseline FDG-PET/CT yields prognostically significant data in patients with mRCC treated with sunitinib. FDG-PET/CT responses were visible in most patients after 4 weeks of therapy. However, it took 16 weeks for the response to become prognostically significant^[34]. Earlier response evaluation with molecular imaging techniques have not yet been published.

In conclusion, functional MR imaging provides promising biomarkers for treatment response. The 3 functional MRI techniques used in this study provided additional information and can be applied in one scan session. This is important for optimal tailoring of personalized therapies in the future. We performed a pilot study in a small and relatively heterogeneous study population including patients pretreated with TKIs and the relationship with PFS has still to be determined. Therefore, further investigation is needed.

References

- [1] Motzer RJ, Hutson TE, Tomczak P, et al. Sunitinib versus interferon alfa in metastatic renal-cell carcinoma. *N Engl J Med* 2007; 356: 115–24. doi:10.1056/NEJMoa065044.
- [2] Motzer RJ, Hutson TE, Tomczak P, et al. Overall survival and updated results for sunitinib compared with interferon alfa in patients with metastatic renal cell carcinoma. *J Clin Oncol* 2009; 27: 3584–90. doi:10.1200/JCO.2008.20.1293.

- [3] Eisenhauer EA, Therasse P, Bogaerts J, *et al.* New response evaluation criteria in solid tumours: revised RECIST guideline (version 1.1). *Eur J Cancer* 2009; 45: 228–47. doi:10.1016/j.ejca.2008.10.026.
- [4] Desar IM, van Herpen CM, van Laarhoven HW, *et al.* Beyond RECIST: molecular and functional imaging techniques for evaluation of response to targeted therapy. *Cancer Treat Rev* 2009; 35: 309–21. doi:10.1016/j.ctrv.2008.12.001.
- [5] Padhani AR, Leach MO. Antivascular cancer treatments: functional assessments by dynamic contrast-enhanced magnetic resonance imaging. *Abdom Imaging* 2005; 30: 324–41.
- [6] Lankester KJ, Taylor JN, Stirling JJ, *et al.* Dynamic MRI for imaging tumor microvasculature: comparison of susceptibility and relaxivity techniques in pelvic tumors. *J Magn Reson Imaging* 2007; 25: 796–805. doi:10.1002/jmri.20881.
- [7] Jain RK. Normalization of tumor vasculature: an emerging concept in antiangiogenic therapy. *Science* 2005; 307: 58–62. doi:10.1126/science.1104819.
- [8] van Laarhoven HW, Rijpkema M, Punt CJ, *et al.* Method for quantitation of dynamic MRI contrast agent uptake in colorectal liver metastases. *J Magn Reson Imaging* 2003; 18: 315–20. doi:10.1002/jmri.10370.
- [9] van Laarhoven HW, Klomp DW, Rijpkema M, *et al.* Prediction of chemotherapeutic response of colorectal liver metastases with dynamic gadolinium-DTPA-enhanced MRI and localized 19F MRS pharmacokinetic studies of 5-fluorouracil. *NMR Biomed* 2007; 20: 128–40. doi:10.1002/nbm.1098.
- [10] Padhani AR, Dzik-Jurasz A. Perfusion MR imaging of extracranial tumor angiogenesis. *Top Magn Reson Imaging* 2004; 15: 41–57. doi:10.1097/00002142-200402000-00005.
- [11] Tofts PS, Brix G, Buckley DL, *et al.* Estimating kinetic parameters from dynamic contrast-enhanced T(1)-weighted MRI of a diffusible tracer: standardized quantities and symbols. *J Magn Reson Imaging* 1999; 10: 223–32. doi:10.1002/(SICI)1522-2586(199909)10:3<223::AID-JMRI2>3.0.CO;2-S.
- [12] Hittmair K, Gomiscek G, Langenberger K, *et al.* Method for the quantitative assessment of contrast agent uptake in dynamic contrast-enhanced MRI. *Magn Reson Med* 1994; 31: 567–71. doi:10.1002/mrm.1910310516.
- [13] Duvvuri U, Poptani H, Feldman M, *et al.* Quantitative T1rho magnetic resonance imaging of RIF-1 tumors in vivo: detection of early response to cyclophosphamide therapy. *Cancer Res* 2001; 61: 7747–53.
- [14] van Laarhoven HW, Fiedler W, Desar IM, *et al.* Phase I clinical and magnetic resonance imaging study of the vascular agent NGR-hTNF in patients with advanced cancers (European Organization for Research and Treatment of Cancer Study 16041). *Clin Cancer Res* 2010; 16: 1351–23.
- [15] Ostergaard L, Weisskoff RM, Chesler DA, *et al.* High resolution measurement of cerebral blood flow using intravascular tracer bolus passages. Part I: Mathematical approach and statistical analysis. *Magn Reson Med* 1996; 36: 715–25. doi:10.1002/mrm.1910360510.
- [16] Ostergaard L, Sorensen AG, Kwong KK, *et al.* High resolution measurement of cerebral blood flow using intravascular tracer bolus passages. Part II: Experimental comparison and preliminary results. *Magn Reson Med* 1996; 36: 726–36. doi:10.1002/mrm.1910360511.
- [17] Span PN, Grebenchtchikov N, Geurts-Moespot J, *et al.* EORTC Receptor and Biomarker Study Group Report: a sandwich enzyme-linked immunosorbent assay for vascular endothelial growth factor in blood and tumor tissue extracts. *Int J Biol Markers* 2000; 15: 184–91.
- [18] Lassau N, Koscielny S, Albiges L, *et al.* Metastatic renal cell carcinoma treated with sunitinib: early evaluation of treatment response using dynamic contrast-enhanced ultrasonography. *Clin Cancer Res* 2010; 16: 1216–25. doi:10.1158/1078-0432.CCR-09-2175.
- [19] Revheim ME, Winge-Main AK, Hagen G, *et al.* Combined positron emission tomography/computed tomography in sunitinib therapy assessment of patients with metastatic renal cell carcinoma. *Clin Oncol (R Coll Radiol)* 2011; 23: 339–43. doi:10.1016/j.clon.2010.11.006.
- [20] Vercellino L, Bousquet G, Baillet G, *et al.* 18F-FDG PET/CT imaging for an early assessment of response to sunitinib in metastatic renal carcinoma: preliminary study. *Cancer Biother Radiopharm* 2009; 24: 137–44. doi:10.1089/cbr.2008.0527.
- [21] Galons JP, Altbach MI, Paine-Murrieta GD, *et al.* Early increases in breast tumor xenograft water mobility in response to paclitaxel therapy detected by non-invasive diffusion magnetic resonance imaging. *Neoplasia* 1999; 1: 113–7. doi:10.1038/sj.neo.7900009.
- [22] Theilmann RJ, Borders R, Trouard TP, *et al.* Changes in water mobility measured by diffusion MRI predict response of metastatic breast cancer to chemotherapy. *Neoplasia* 2004; 6: 831–7. doi:10.1593/neo.03343.
- [23] Patterson DM, Padhani AR, Collins DJ. Technology insight: water diffusion MRI—a potential new biomarker of response to cancer therapy. *Nat Clin Pract Oncol* 2008; 5: 220–33. doi:10.1038/ncponc1073.
- [24] Schraml C, Schwenzer NF, Martirosian P, *et al.* Diffusion-weighted MRI of advanced hepatocellular carcinoma during sorafenib treatment: initial results. *AJR Am J Roentgenol* 2009; 193: W301–W307. doi:10.2214/AJR.08.2289.
- [25] Jain R, Scarpance LM, Ellika S, *et al.* Imaging response criteria for recurrent gliomas treated with bevacizumab: role of diffusion weighted imaging as an imaging biomarker. *J Neurooncol* 2010; 96: 423–31. doi:10.1007/s11060-009-9981-6.
- [26] Pope WB, Kim HJ, Huo J, *et al.* Recurrent glioblastoma multiforme: ADC histogram analysis predicts response to bevacizumab treatment. *Radiology* 2009; 252: 182–9. doi:10.1148/radiol.2521081534.
- [27] Koh DM, Blackledge M, Collins DJ, *et al.* Reproducibility and changes in the apparent diffusion coefficients of solid tumours treated with combretastatin A4 phosphate and bevacizumab in a two-centre phase I clinical trial. *Eur Radiol* 2009; 19: 2728–38. doi:10.1007/s00330-009-1469-4.
- [28] Gerstner ER, Chen PJ, Wen PY, *et al.* Infiltrative patterns of glioblastoma spread detected via diffusion MRI after treatment with cediranib. *Neuro Oncol* 2010; 12: 466–72.
- [29] Hahn OM, Yang C, Medved M, *et al.* Dynamic contrast-enhanced magnetic resonance imaging pharmacodynamic biomarker study of sorafenib in metastatic renal carcinoma. *J Clin Oncol* 2008; 26: 4572–8. doi:10.1200/JCO.2007.15.5655.
- [30] Flaherty KT, Rosen MA, Heitjan DF, *et al.* Pilot study of DCE-MRI to predict progression-free survival with sorafenib therapy in renal cell carcinoma. *Cancer Biol Ther* 2008; 7: 496–501.
- [31] Machiels JP, Henry S, Zanetta S, *et al.* Phase II study of sunitinib in recurrent or metastatic squamous cell carcinoma of the head and neck: GORTEC 2006–01. *J Clin Oncol* 2010; 28: 21–8. doi:10.1200/JCO.2009.23.8584.
- [32] Zhu AX, Sahani DV, Duda DG, *et al.* Efficacy, safety, and potential biomarkers of sunitinib monotherapy in advanced hepatocellular carcinoma: a phase II study. *J Clin Oncol* 2009; 27: 3027–35. doi:10.1200/JCO.2008.20.9908.
- [33] Murukesh N, Dive C, Jayson GC. Biomarkers of angiogenesis and their role in the development of VEGF inhibitors. *Br J Cancer* 2010; 102: 8–18. doi:10.1038/sj.bjc.6605483.
- [34] Kayani I, Avril N, Bomanji J, Chowdhury S, *et al.* Sequential FDG-PET/CT as a Biomarker of Response to Sunitinib in Metastatic Clear Cell Renal Cancer. *Clin Cancer Res* 2011; 17: 6021–8. doi:10.1158/1078-0432.CCR-10-3309.